[Veena* *et al.*, 5(10): October, 2016]
IC™ Value: 3.00

ISSN: 2277-9655
Impact Factor: 4.116
CODEN: IJESS7

IJESRT
INTERNATIONAL JOURNAL OF ENGINEERING SCIENCES & RESEARCH TECHNOLOGY

STUDY ON SIMILARITY SOLUTIONS FOR MHD VISCO-ELASTIC FLOW WITH HEAT AND MASS TRANSFER OVER A PERMEABLE STRETCHING SHEET EXTRUDED IN A CROSS COOLING STREAM WITH HEAT SOURCE/SINK

P H Veena*, Neelkamal S, A Mallikarjungouda, V K Pravin
* Dept. of Mathematics, Smt. V.G. College for Women, Gulbarga, Karnataka, India
Dept. of Mathematics, Gulbarga University, Gulbarga, Karnataka, India
Dept. of Mathematics, A S M College for Women, Bellary, Karnataka, India
Dept. of Mech. Engg., P.D.A. College of Engg., Gulbarga, Karnataka, India

DOI: 10.5281/zenodo.163075

ABSTRACT
Study of similarity solutions for flow with heat and mass transfer characteristics on a continuous accelerated sheet extruded in a cross-cooling steady stream of an incompressible visco-elastic (Walter's liquid B') fluid is a analysed. An industrial application of this type of problem is the cooling of extruded plastic sheet during formation process.

The effects of various physical parameters encountering in the study like visco-elasticity, Reynold's number, Prandtl number Shrewood number, and velocity ratio are investigated in an appropriate form using suitable analytical methods.

Results for skin friction, heat transfer co-efficient and mass transfer co-efficient are obtained. The power law constant for wall temperature and wall concentration have an effective influence on heat and mass transfer mechanics.

KEYWORDS: Walter's liquid, heat transfer, mass transfer, magnetohydrodynamics, cooling stream, similarity solutions.

INTRODUCTION
Mathematical and numerical studies of so-called continuous moving surface flow due to a stretching sheet have received a good amount of attention in the literature.

The study of two dimensional boundary layer flow with heat and mass transfer over a stretching surface have many industrial applications in different areas. Heat and mass transfer analysis over a stretching sheet is of much practical interest due to its abundant applications in several manufacturing processes and they led to renewed interest among young researchers to investigate boundary layer flow over a stretching sheet with various physical consequences.

Many materials such as polymer solutions or melts, drilling mud, clastomers, certain oils and greases and many other emulsions are classified as non-Newtonian fluids. In view of the above applications, Sakiadis [1] initiated the study of boundary layer flow over a continuous solid surface moving with constant speed. McCromack and Crane [2] provided a comprehensive discussion on boundary layer flow caused by stretching of an elastic sheet moving in its own plane with linear velocity. Khan et. al., [3] have obtained appropriate similarity solutions of visco-elastic boundary layer flow with heat transfer over an exponential stretching sheet . Cortell [4] have studied visco-elastic flow with CST and PST cases in heat transfer analysis. Bataller [5] also studied the similar problem of [4] for PST and PHF cases. Analytical results were carried out by Vajravelu et. al., [6] who took into account the effects of viscous dissipation and internal heat generation. An analysis of thermal boundary layer in an MHD fluid over a linearly stretching sheet in the presence of magnetic field with viscous and joules dissipation and internal heat generation was carried out by Chaim [7]. Recently, Sajid et. al., [8] have studied the analytical solutions for MHD flow and heat transfer in an third order fluid over a stretching sheet. Tak and Lodha [9] made an analysis on flow and heat transfer due to a stretching surface.

Ganga et. al., [10] have investigated about the non-linear hydromagentic flow and heat transfer due to stretching porous surface with PHF and joule dissipation Ganga et. al., [11] also made a study on the effects of viscous, dissipation on MHD flow with heat and mass transfer past a porous stretching surface.

Chung Liu [12] made a detail analysis on flow and heat transfer in an MHD fluid of second grade over a stretching sheet with viscous dissipation and internal heat generation. Besides a great deal of work has been carried out to find the similarity solution of visco-elastic fluid flow over an impervious stretching boundary [13, 14, 15, 16].

Subhas and Veena [17] studied the problem of Vajravelu [6] by including the effects of frictional heating and internal heat generation.

Hassanien [18] developed the boundary layer solutions for the flow and heat transfer on continuous flat surface in parallel free stream of power law fluid. Sarma and Rao [19] and Vajravelu and Roper [20] analysed the effects of work due to deformation in the energy equation for negative and positive material constant α respectively. Again the flow and heat transfer of a second order fluid on a continuous flat surface moving in a parallel free stream was studied by Hassanien [21]. Hassanian [22] made an analysis on the flow and heat transfer in a visco-elastic fluid over a stretching sheet in a cross cooling stream. He showed that the velocity distribution along the transverse direction increases with increasing values of visco-elastic parameter k_1 for the case $u_{\delta m} > u_{wm}$ and the opposite effects are observed for the case $u_{wm} > u_{\delta m}$. Neil [23] imposed a technical note on the similarity solutions for flow over an impermeable sheet . The same problem was studied by Raptis and Perdikis [24] over a non-linearly stretching sheet.

All the above studies are restricted only to the flow of visco-elastic fluid past a stretching with heat transfer analysis. Thus motivated by the above analyses in the present paper, the study of steady cross-cooling two dimensional flow of an incompressible visco-elastic fluid (Walter's liquid B' model) is considered whose constitutive equation based on the postulate of fading memory suggested by Coleman and Noll [25].

Further the combined effect of the stretching or accelerating phenomena during the sheet formation process and the acceleration rate of cooling stream at the edge of boundary layer are studied. Heat and mass transfer analyses are carried out. I n energy transfer internal heat generation is considered. A simple and suitable normalization technique is employed which enables us to clarify the effects of Reynolds number , Prandtl number and Shrewood number for all possible combinations of the velocity gradient $f_{\eta\eta}(0)$, temperature gradient $\theta_\eta(0)$ and concentration gradient $-\phi_\eta(0)$ both for the sheet and the cooling stream on the values of skin friction co-efficient, heat transfer co-efficient and the mass transfer co-efficient. Heat and mass transfer from a sheet with constant or variable surface temperature simulating the cooling process are also considered in the study.

MATHEMATICAL ANALYSIS

An incompressible second order fluid with constitutive equation given by author [25] is considered and which is given as

$$T = -PI + \mu A_1 + \alpha_1 A_2 + \sigma_2 A_1^2 \qquad \text{...(i)}$$

where all notations have usual meanings and are noted in nomenclature. The kinematic Rivlin-Erickson tensors A_1 and A_2 are defined as.

$$A_1 = L + L^T \qquad \text{...(ii)}$$

$$A_2 = \frac{dA_1}{dt} + A_1 L + L^T A_1 \qquad \text{...(iii)}$$

where $\frac{d}{dt}$ is the material derivative and $L = \nabla V$. Since the fluid is of second grade, it has to satisfy the Clausiues-Dehum in- equality for all motions and the assumption that the specific Helmotz free energy of the fluid is minimum when it is locally at rest. Then the requirements for the moduli are

$\mu \geq 0, \quad \alpha_1 > 0 \text{ and } \alpha_1 + \alpha_2 = 0$ …(iv)

where the sign of α_1 has been a subject of controversy. In this view a critical review is already made by Dunn and Rajgopal [26] and the fluids of second grade with negative α_1 may result in physically impossible flow situation. Model (i) considered by [25] displays normal stress difference in shear flow and is an approximation to a simple fluid in the sense of retardation. This model is applicable to some dilute polymer solutions at the low rates of shear. The physical model is described as below. An endless moving sheet extruded from a slit or extrusion die with a surface velocity $u_u(x)$ increasing through the zone of deformation from zero to a final wind-up velocity u_{um}. The sheet is extruded in a uniform cross flow of a cooling fluid. The extrusion conditions are defined as in nomenclature at the boundary layer edge. Laminar boundary layer flow usually occurs over a length of about 0.5m from the extrusion die. This is however, the zone over which the major part of the stretching process, heat transfer takes place. The obtained solution is valid for points down stream of 0" the point of maximum sheet thickness where the axial velocity has become approximately uniform over the cross-section of the extruded material upto the order of 0" of solidification after which the extruded sheet becomes completely solid with uniform thickness and speed.

The effects of spatial variations viz. $\bar{\rho}, \bar{\mu} \text{ and } \bar{k}_f$ are negligible as considered in [22]. The velocity components u & v are normalized by the largest velocity in the boundary layer as reference velocity $\bar{u}_r$ at $\bar{x} = L$ - the characteristic length which is defined as

$$\bar{u}_r = \begin{cases} \bar{u}_{\delta m} & \text{if } \bar{u}_{wm} < \bar{u}_{\delta m} \\ u_{wm} & \text{if } \bar{u}_{wm} > \bar{u}_{\delta m} \end{cases} \quad \ldots(v)$$

The physical model Fig. (I) which is a symmetrical figure and thus only one half of it is shown can be divided into two regions.

a. The boundary layer along the extruded sheet and
b. The external frictionless potential flow outside the boundary layer.

Thus considering the stream function of the potential flow as

$$\Psi_e = u_{\delta m}\, xy \quad \ldots(vi)$$

The velocity distribution of the flow is given by

$$u_e = u_{\delta m}\, x; \quad v_e = -u_{\delta m}\, y \quad \ldots(vii)$$

and the relation between the cooling stream velocity at duct exit v_0 and the maximum velocity $u_{\delta m}$ at the boundary layer edge is given by [22] as

$$v_0 = -u_{\delta m}\, y_0 \quad \ldots(viii)$$

and the sheet speed in the deformation zone is approximated as

$$u_w = u_{wm} x, \; o \leq x \leq 1 \quad \ldots(ix)$$

where $\bar{x}$ is the normalized distance. Now defining the Reynolds number as

$$R_e = \frac{\bar{u}_\alpha \bar{L}}{\bar{v}} = O\left(\frac{1}{\epsilon^2}\right), \; \epsilon \leq\leq 1 \quad \ldots(x)$$

Introducing the following dimensionless variables we obtain the resulting dimensionless boundary layer equations developed along the extruded sheet.

$$x = \bar{x}/\bar{L} = O(1); \; y = \bar{y}/\bar{L} = O(\epsilon); \; u = \bar{u}/\bar{u}_r = O(1),$$

$$v = \frac{\bar{v}}{\bar{u}_r} = O(\epsilon); \; T = \frac{(\bar{T} - \bar{T}_\infty}{\bar{T}_0 - \bar{T}_\infty)} = O(1); \; C = \frac{\bar{C} - \bar{C}_\infty}{\bar{C}_0 - \bar{C}_\infty} = O(1) \quad \ldots(xi)$$

$$\frac{\partial u}{\partial x} + \frac{\partial v}{\partial y} = 0 \quad \ldots(1)$$

$$u\frac{\partial u}{\partial x}+\frac{\partial u}{\partial y}=-\frac{\partial p}{\partial x}+\frac{1}{\mathrm{Re}}\left(\frac{\partial^2 u}{\partial y^2}\right)-\alpha_1\left[\frac{\partial}{\partial x}\left(u\frac{\partial^2 u}{\partial y^2}\right)+\frac{\partial u}{\partial y}\cdot\frac{\partial^2 v}{\partial y^2}+v\frac{\partial^3 u}{\partial y^3}\right] \quad \ldots(2)$$

$$u\frac{\partial T}{\partial x}+v\frac{\partial T}{\partial y}=\frac{1}{\mathrm{Pr\,Re}}\frac{\partial^2 T}{\partial y^2}+Q'(T-T_\infty) \quad \ldots(3)$$

$$u\frac{\partial c}{\partial x}+v\frac{\partial c}{\partial y}=\frac{1}{Sc\,\mathrm{Re}}\frac{\partial^2 c}{\partial y^2} \quad \ldots(4)$$

with boundary conditions

$$y=0;\ u=u_w, v=0,$$

$$\bar{T}_s(x)=\bar{T}_\infty+(\bar{T}_0-\bar{T}_\infty)x^l, 0\le x\le 1$$

$$\bar{C}_s(x)=\bar{C}_\infty+(\bar{C}_0-\bar{C}_\infty)x^l \quad \ldots(5)$$

$$y=\delta,\ u\to u_\delta,\ T\to T_\infty,\ C\to C_\infty \quad \ldots(6)$$

where $\alpha_1=\frac{\alpha}{\rho L^2}$, $\nu=\frac{\mu}{\rho}$, $P_r=\frac{\mu C_p}{\alpha_1}$, $Sc=\frac{\nu}{D}$

and the pressure gradient along x is given by $\frac{\partial p}{\partial x}=-u_\delta\frac{du_\delta}{dx}$ …(7)

where $\Psi(x,y)=\frac{\bar{\psi}}{(\bar{u},L)}=0(\in)$, $u=\frac{\partial\psi}{\partial y}$, $v=\frac{-\partial\psi}{\partial x}$ …(8)

Refining the following similarity variable and stream transformation as

$$\eta(x,y)=\sqrt{\mathrm{Re}}\,y=O(1);\ f(\eta)=\sqrt{\mathrm{Re}}\,\psi(x,y)\,|\,x=O(1)$$

$$\theta(\eta)=\frac{\bar{T}-\bar{T}_\infty}{\bar{T}_w-\bar{T}_\infty}=O(1);\ \phi(\eta)=\frac{\bar{C}-\bar{C}_\infty}{C_w-C_\infty}=O(1) \quad \ldots(9)$$

substituting equations (9) into equations (2), (3) and (4) we get

$$f_\eta^2-ff_{\eta\eta}=f_{\eta\eta}-k_1[2f_\eta f_{\eta\eta\eta}-f_{\eta\eta}{}^2-ff_{\eta\eta\eta\eta}]+u_{\delta m}^2 \quad \ldots(10)$$

where $\mathrm{Pr}=\frac{\mu c_p}{\alpha_1}$ *and* $Q=\frac{Q'\nu}{\alpha_1}$

$$\theta_{\eta\eta}+P_r f\theta'_\eta+(lf_\eta+Q)\theta=0 \quad \ldots(11)$$

$$\phi_{\eta\eta}+Scf\,\phi_\eta+Scl\,f_\eta\,\phi=0 \quad \ldots(12)$$

where suffix η denotes differentiation w.r.t it and $k_1=\frac{\alpha_1 u_r L}{\nu}$ is the visco-elastic parameter.

The velocity components u and v converts to

$$u=xf_\eta;\ \ v=\frac{f}{\sqrt{\mathrm{Re}}} \quad \ldots(13)$$

Then the boundary conditions (5) and (6) become

$$f(0)=0,\ f_\eta(0)=u_{um};\ f_\eta(\eta_\delta)=u_{\delta m};\ \theta(0)=1, \theta(\eta_\delta)=0$$

$$f_{\eta\eta}(\eta_\delta)=0;\ \phi(0)=1,\ \phi(\eta_\delta)=0 \quad \ldots(14)$$

If $u_{\delta m} > u_{um}$ then $u_{\delta m} = 1$, $o \le u_{um} \le 1$ …(14a)

If $u_{um} > u_{\delta m}$ then $u_{um} = 1$, $o \le u_{\delta m} \le 1$ …(14b)

Equation (10) can be recognized as the Hiemenz flow [ ] and it can be reduced to Falkner-skan flow of second grade fluid [ ] when $u_{\delta m} = 0$ subjected to the boundary conditions

$$f(0) = 0,\ f_\eta(0)=0, f_\eta(\eta_\delta)=1 \text{ and } f_{\eta\eta}(\eta_\delta)=0 \quad \ldots(15)$$

ANALYTICAL SOLUTION

In order to get the exact analytical solution of equation (10) which is non-Newtonian model and is applicable to dilute polymer solutions, applying retarded-motion expansion by assuming $k_1 \le \le 1$ and expanding the velocity function f with respect to visco-elastic parameter k_1 as

$$f = f_0 + k_1 f_1 + k_1^2 f_2 + \quad \ldots(16)$$

substituting the above expansion in equation (10) and considering the first two terms of the series expansion, we obtain

$$f_{0\eta}^2 + f_0 f_{0\eta\eta} = f_{0\eta\eta\eta} + u_{\delta m}^2 \quad \ldots(17)$$

$$f_{1\eta\eta\eta} + f_1 f_{0\eta\eta} + f_0 f_{1\eta\eta} - 2f_{0\eta}f_{1\eta} = +\left[2f_{0\eta}f_{0\eta\eta\eta} + f_{0\eta\eta}^2 + f_0 f_{0\eta\eta\eta\eta}\right] \quad \ldots(18)$$

$$\theta_{\eta\eta} + P_r f\theta_\eta + P_r\left(lf_\eta + Q\right)\theta = 0 \quad \ldots(19)$$

$$\phi_{\eta\eta} + Sc\, f\phi_\eta + Sc\, lf_\eta\, \phi = 0 \quad \ldots(20)$$

with the following boundary conditions

$$f_0(0)=0,\ f_{0\eta}(0)=u_{um},\ f_{0\eta}(\eta_\delta)=0 \quad \ldots(21)$$

$$\theta(0)=1;\ \theta(\eta_\delta)=0 \quad \ldots(22)$$

$$\phi(0)=1;\ \phi(\eta_\delta)=0 \quad \ldots(23)$$

Now it is interesting to study that the exact analytical solution of equation for $u_{\delta m} = 0$ is obtained as

$$f(\eta) = (1-\exp(-\eta)) \quad for\ \ k_1 = elastic\, parameter = 0 \quad \ldots(24)$$

on the other hand Troy et. al., [ ] obtained the solution of equation [10] as

$$f(\eta) = \left[\frac{1-e^{-\beta\eta}}{\beta}\right],\ \beta = \frac{1}{\sqrt{1-k_1}} \quad \ldots(25)$$

satisfying the boundary conditions (14) and gives the new velocity components

$$u = xe^{-\beta\eta}; \quad \ldots(26)$$

$$v = \frac{(1-\exp(-\beta\eta))}{\beta\,\mathrm{Re}} \quad \ldots(27)$$

To solve energy equation (19) and mass diffusion equation (20), introducing the new change of variables

$$\xi = \frac{-P_r}{\alpha^2}\bar{e}^{\alpha\eta} \quad \ldots(28)$$

$$\zeta = -\frac{Sc}{\alpha^2}\bar{e}^{\alpha\eta} \quad \ldots(29)$$

Substituting (3), (28) , (29) and f(η) in equations (19) and (20) respectively they yield to the following form of equations.

$$\xi\theta_{\xi\xi} + \left(1 - \frac{P_r}{\alpha^2} - \xi\right)\theta_\xi + P_r\left(l+Q\right)\theta = 0 \quad \ldots(30)$$

$$\zeta\,\phi_{\zeta\zeta} + \left(1 - \frac{Sc}{\alpha^2} - \zeta\right)\phi_\zeta + Sc\, l\,\phi = 0 \quad \ldots(31)$$

ISSN: 2277-9655
Impact Factor: 4.116
CODEN: IJESS7

The boundary conditions are converted to

$$\theta\frac{(-\Pr)}{\alpha^2}=1;\ \theta(0)=0 \qquad \ldots(32)$$

$$\phi\left(-\frac{Sc}{\alpha^2}\right)=1;\ \phi(0)=0 \qquad \ldots(33)$$

Now the solutions of both the equations (30) and (31) with respect to the boundary condition s (32) and (33) interms of η are obtained and expressed interms of confluent hyper geometric (Kummer's) functions [29] as follows

$$\theta(\eta)=\bar{e}\frac{P_r\eta}{\alpha}.\ F\frac{\left[\left(\frac{P_r}{\alpha^2}-l+1,\frac{P_r}{\alpha^2}+2,\frac{-P_r}{\alpha^2}\right)\right]}{F\left[\frac{P_r}{\alpha^2}-l,\frac{P_r}{\alpha^2}-1,\frac{-P_r}{\alpha^2}\right]} \qquad \ldots(34)$$

$$\phi(\eta)=e^{-\frac{Sc}{\alpha}\eta}\frac{F\left[\frac{Sc}{\alpha^2}-l+1,\frac{Sc}{\alpha^2}+2,\frac{-Sc}{\alpha^2}e^{-\alpha\eta}\right]}{F\left[\frac{Sc}{\alpha^2}-l,\frac{Sc}{\alpha^2}-1,\frac{-Sc}{\alpha^2}\right]} \qquad \ldots(35)$$

The non dimensional wall temperature gradient and wall concentration gradient derived from equations (34) and (35) respectively as

$$\theta_\eta(0)=-P_r+\frac{P_r(P_r-l+1)}{(P_r+1)}\frac{F[P_r-l+1,P_r+2,-P_r]}{F[P_r-l,P_r-1,-P_r]} \qquad \ldots(36)$$

$$\phi_\eta(0)=-Sc+\frac{Sc(Sc-l+1)}{(Sc+1)}\frac{F[Sc-l+1,Sc+2,-Sc]}{F[Sc-l,Sc-1,-Sc]} \qquad \ldots(37)$$

Heat transfer co-efficient

The local Nusselt number Nux along the sheet is derived as

$$Nux=(\partial T/\partial y)y=0=-\theta_\eta(0)\sqrt{\mathrm{Re}} \qquad \ldots(38)$$

Mass transfer co-efficient

The local Shrewood number Sh along the sheet is defined as

$$Sh=(\partial C/\partial y)y=o=-\phi_\eta(0)\sqrt{\mathrm{Re}} \qquad \ldots(39)$$

The local wall heat flux and mass flux can be derived and expressed as

$$q_w=-k_1\left(\frac{\xi}{P_r}\right)^{P_r}\frac{F[\Pr-l,P_r+1,\ \xi]}{F[P_r-l,P_r-1,-P_r]} \qquad \ldots(40)$$

$$h_w=-\alpha_1\left(\frac{\zeta}{Sc}\right)^{Sc}\frac{F[Sc-l,Sc+1,\zeta]}{F[Sc-l,Sc-1,-Sc]} \qquad \ldots(41)$$

Skin friction coefficient

The wall shear stress τ_w can be expressed interms of dimensionless skin-friction coefficient C_f as0

$$C_f=\frac{\bar{\tau}_w}{(\rho\bar{u}_r^2)}=(\partial u/\partial y)y=0=\frac{x}{\sqrt{\mathrm{Re}}}\ f_{\eta\eta}(0)(1+3u_{um}k_1)$$

ISSN: 2277-9655
Impact Factor: 4.116
CODEN: IJESS7

Nomenclature

A_1, A_2	=	First and second Rivlin-Erickson tensors
C_p	=	Specific heat at constant pressure
C_f	=	Skin friction coefficient
D	=	Diffusivity
f	=	Dimensionless velocity
F (a,b,z)	=	Kummers functions
k	=	visco-elasticity
l	=	Characteristic length
$\overline{L}$	=	Characteristics length
L	=	∇ V
Nu	=	Nusselt number
p	=	Pressure/parameter
P_r	=	Prandtl number
q	=	heat source
Q	=	Internal heat source parameter in equation (3)
Re	=	Reynolds number
Sc	=	Schimidt number
Sh	=	Shrewood number
r, w, u	=	Suffixes for velocity
T	=	Temperature
T_w	=	Wall temperature
T_∞	=	Ambient temperature
$T_{\overline{T}_o}$	=	Cauchy stress tensor solidification temperature
u, v, u_r	=	Velocity components
V	=	Velocity vector
x,y	=	Co-ordinate system
k_1	=	Elastic parameter

Greek symbols

α^*	=	Dimensionless internal parameter
α	=	Positive root of cubic equation
α_1, α_2	=	Material constant
δ	=	Boundary layer thickness
ϕ	=	Dimensionless concentration variable
θ	=	Dimensionless temperature variable
η	=	Dimensionless similarity variable
μ	=	Dynamic viscosity
ν	=	Kinematic viscosity
ρ	=	Density
ξ	=	New dimensionless change of temperature variable
ζ	=	New dimensionless change of concentration variable
ψ	=	Stream function
$\overline{\tau}_w$	=	Wall shear stress
τ	=	Dimensionless shear stress
$\overline{u}_{wm}$	=	Windup speed
$\overline{u}_{\delta m}$	=	Final reference speed
$\overline{T}_0$	=	Solidification temperature
$\overline{T}_\infty$	=	Environmental
t(x)	=	Sheet thickness

ISSN: 2277-9655
Impact Factor: 4.116
CODEN: IJESS7

$u_w(x)$	=	Sheet velocity
$u_{\delta m}$	=	Reference velocity
u_∞	=	Free stream velocity
$\frac{d}{dt}$	=	material time derivative
U_{wm}	=	Windup velocity

RESULTS AND DISCUSSION

In order to have a physical point of view of the problem, numerical calculations were carried out for different values of visco-elastic parameter k_1, Prandtl number P_r, Schimidt number Sc and Reynolds number Re.

The dimensionless and transverse velocity profiles $f_\eta(\eta) \& f(\eta)$ for five different cases of $u_{um} > u_{\delta m}$ and $u_{um} < u_{\delta m}$ are presented in figures 1 and 2. It is observed that the slopes of the corresponding curves in Fig. 1 at η = 0, to η = 8 rise steadily for the case $u_{um} < u_{\delta m}$ but the opposite effect are observed for $u_{um} > u_{\delta m}$, which explains that the boundary layer thickness is uniform for each case (u_{um}, $u_{\delta m}$). It is also revealed from Fig. (1) that the wall shear stress is larger for $u_{um} < u_{\delta m}$ than for $u_{um} > u_{\delta m}$.

Fig. 2 shows that the normal velocity ν acts always towards the extruded surface and for the same Reynolds number wall shear stress is larger for $u_{um} < u_{\delta m}$ than $u_{um} > u_{\delta m}$.

Fig. 3 dipicts the dimensionless temperature distribution within the boundary layer for the same four cases of (u_{um}, $u_{\delta m}$) for P_r = 3 and the case of uniform wall temperature l = 0. The nature of the curves measures the wall heat transfer and shows the thickness of the thermal boundary layer as $\bar{T} \to \bar{T}_\infty \ to \ \theta(\infty) = O.$

Fig. 4a. is the presentation of friction factor $f_{\eta\eta}(0)$ for two values of visco-elastic parameter k_1 = 0.0 and $k_{1=}$ 0.2. From the figure it is observed that for the four possible combinations of u_{um} and $u_{\delta m}$, the curves lie in two groups. The upper two curves refers the value range $u_{um} < u_{\delta m}$ and the lower two curves are for $u_{um} > u_{\delta m}$.

The values of friction co-efficient for a given value of Re depends only on the normalized velocity difference | u_{um}-$u_{\delta m}$ |, but also on that of the sheet and the cooling stream which moves faster. Skin friction co-efficient is larger from $u_{um} < u_{\delta m}$ than for $u_{um} > u_{\delta m}$ for non-Newtonian and Newtonian fluid flows which is because of the pressure gradient along the sheet is large.

Fig. 4b. is plotted for the skin friction co-efficient $f_{\eta\eta}(0)$ Vs Reynolds number for various values of visco-elastic parameter k_1. From the figure it is apparent that the curves are independent of the magnitudes of the velocities whose effects are contained in the Reynolds number Re and the velocity difference.

In fig. 5 the graph of temperature profiles θ(η) is drawn for various values of Prandtl number Pr. It reveals from the figure that an increase in Prandtl number is associated with a decrease in temperature distribution within the thermal boundary layer for the same four cases of ($u_{um} < u_{\delta m}$).

Fig. 6 is drawn to explain the effect of Pr on wall temperature gradient $\theta_\eta(O)$ for the same value of Reynolds number Re=100. From the figure we can see that the rate of heat transfer decreases for increase in both Prandtl number and wall temperature parameter l. Temperature gradient is negative for all values of wall temperature parameter. Physically it means that heat flows from the surface to the ambient fluid. This is consistent with the fact that the thermal boundary layer thickness decrease with increasing Prandtl number and is well in agreement with the results of [6] and [22].
Fig. 7 is the graph of $\theta_\eta(0)$ vs. wall temperature parameter l. when l =1, there is no heat transfer between the surface and the ambient fluid, where $l < 1$, $\theta_\eta(0)$ is positive and $l > 1$, $\theta_\eta(0)$ is negative.

ISSN: 2277-9655
Impact Factor: 4.116
CODEN: IJESS7

Fig. 8 is the representation of concentration profiles $\phi(\eta)$ for different values of Schimidt number Sc. Increase in Schimidt number decreases the concentration distribution within the boundary layer.

Fig. 9 display the variation of rates of mass transfer $\phi_\eta(0)$ against wall concentration parameter l for the same 4 sets of (u_{um}, < $u_{\delta m}$). The concentration gradient of the fluid reduces with increase in l.

Fig. 10 illustrates the graph of concentration gradient $\phi_\eta(0)$ against Schimidt number Sc. It is observed from the figure that for increasing values of Sc, the concentration distribution steadily decreases within the concentration boundary layer.

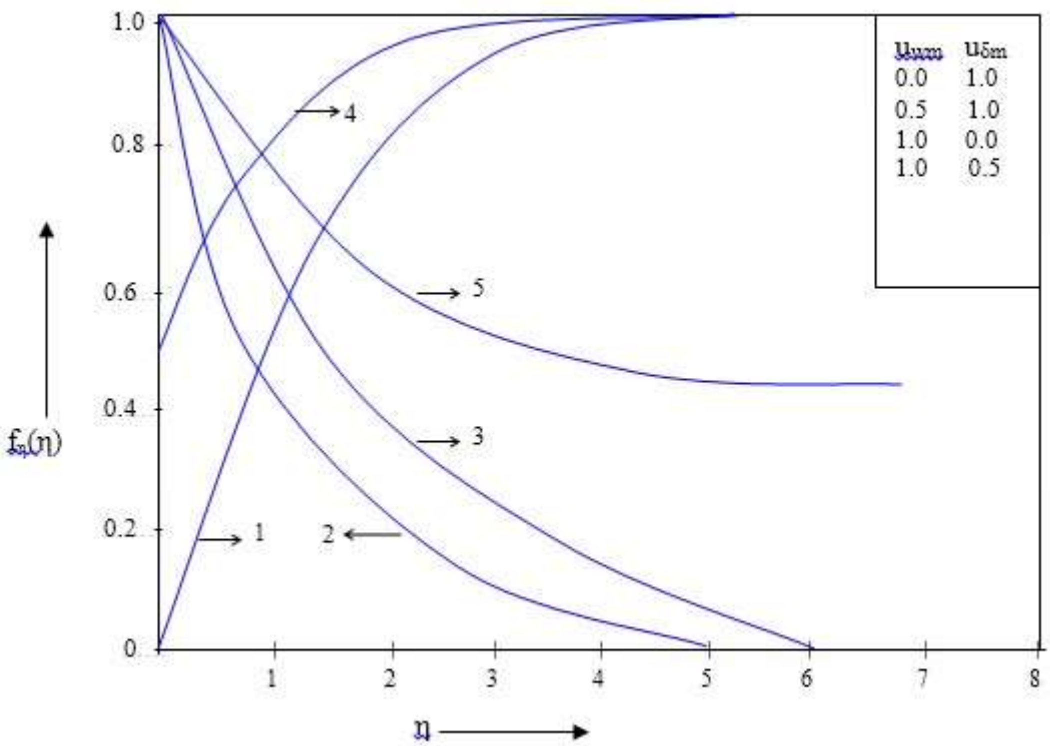

Fig1. Graph of longitudinal velocity distribution $f_\eta(\eta)$ Vs. η for visco-elastic parameter k_1= 0.2 , α = 0.375

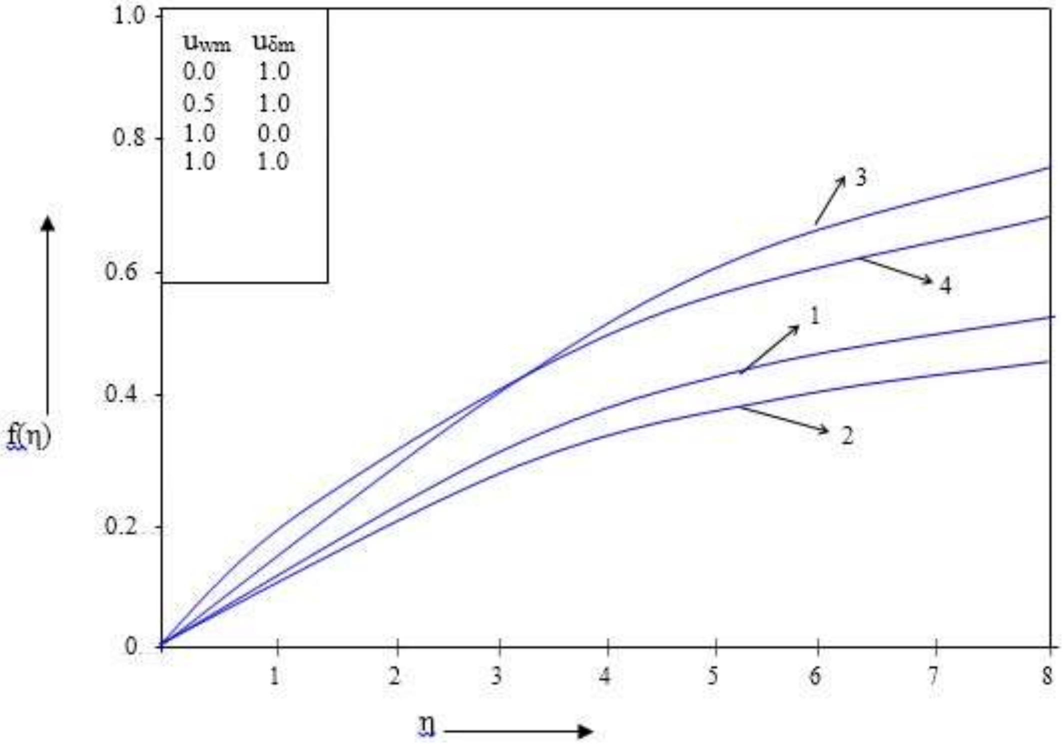

Fig2. Graph of transverse velocity distribution f(η) Vs. η for the value of visco-elastic parameter k_1= 0.2 , α = 0.375

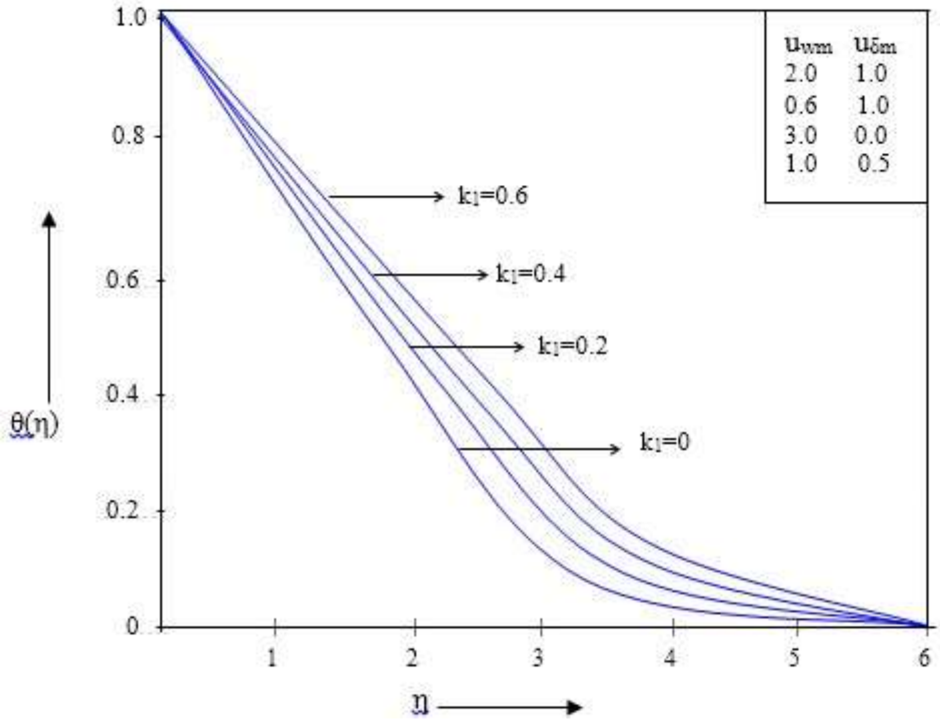

Fig3. Graph of temperature profiles θ(η) Vs. η for the value Pr = 3, Q = 0.5, Re = 100

ISSN: 2277-9655
Impact Factor: 4.116
CODEN: IJESS7

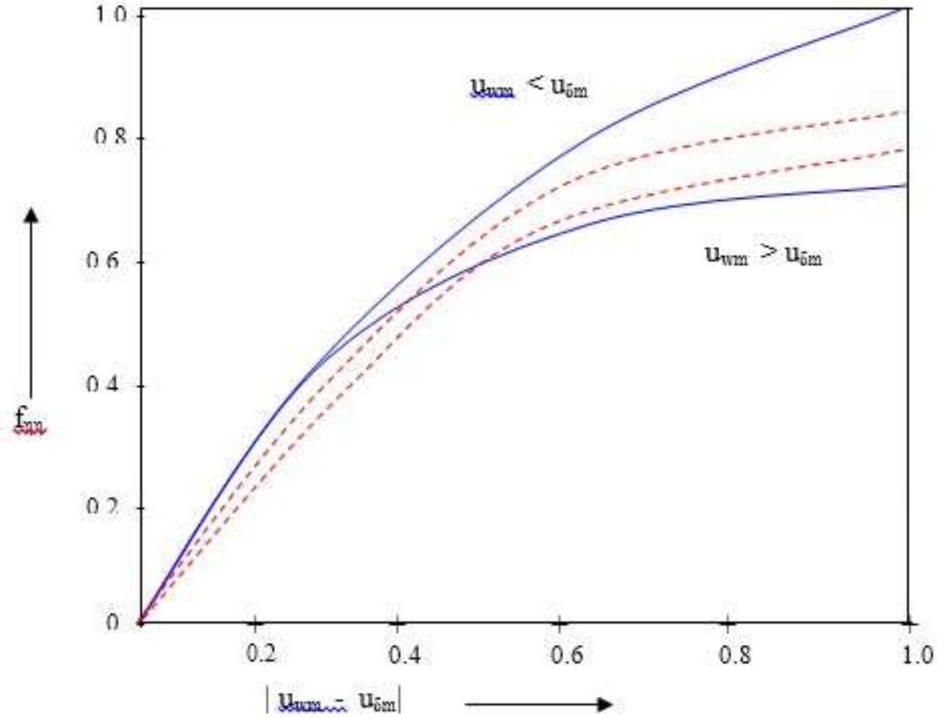

Fig4a. Graph of skin friction gradient $f_{\eta\eta}(0)$ Vs. the velocity difference | u_{wm} - $u_{\delta m}$ | for visco-elastic parameter k_1 = 0.0 and k_1 = 0.2, Re = 100

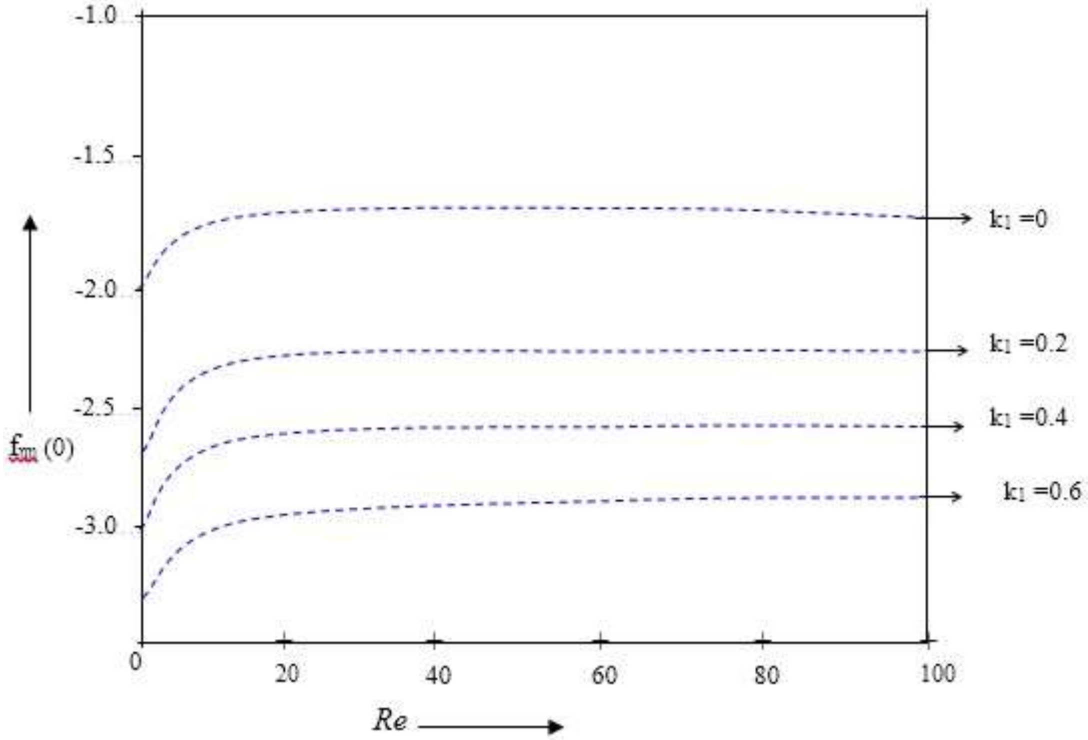

Fig4b. Graph of Skin friction co-eficient $f_{\eta\eta}$ (0) Vs. Reynolds number Re for various values of visco-elastic parameter.

ISSN: 2277-9655
Impact Factor: 4.116
CODEN: IJESS7

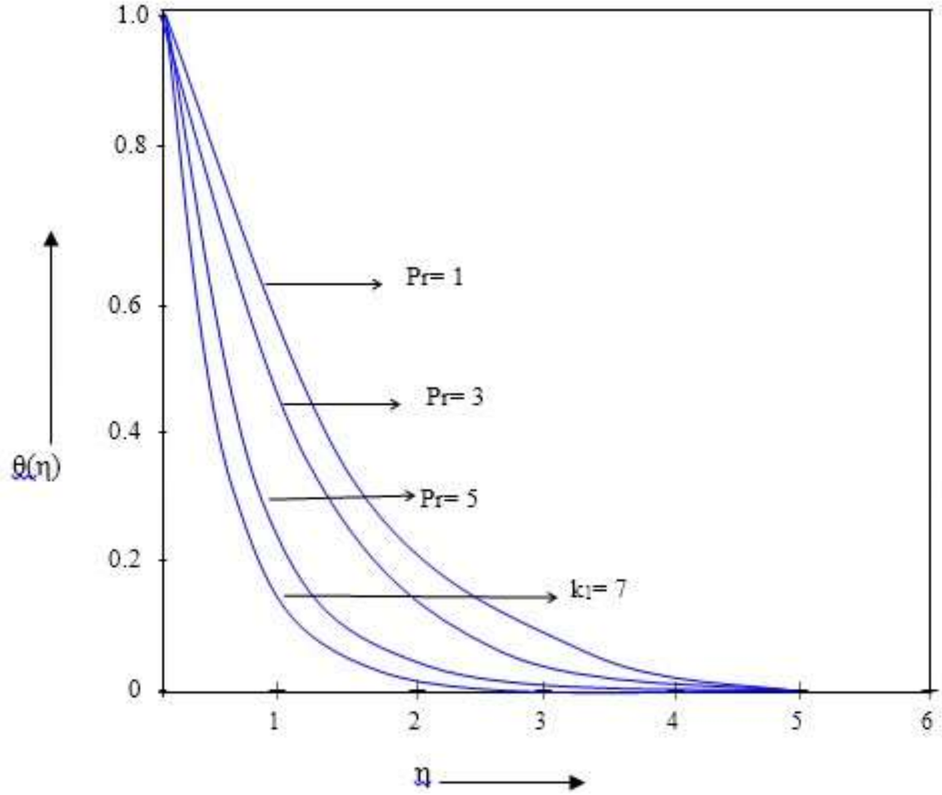

Fig5. Graph of temperature profiles θ(η) Vs. η for visco-elastic parameter k_1***=0.2, Q=0.5, Pr = 1, 3,5,7***

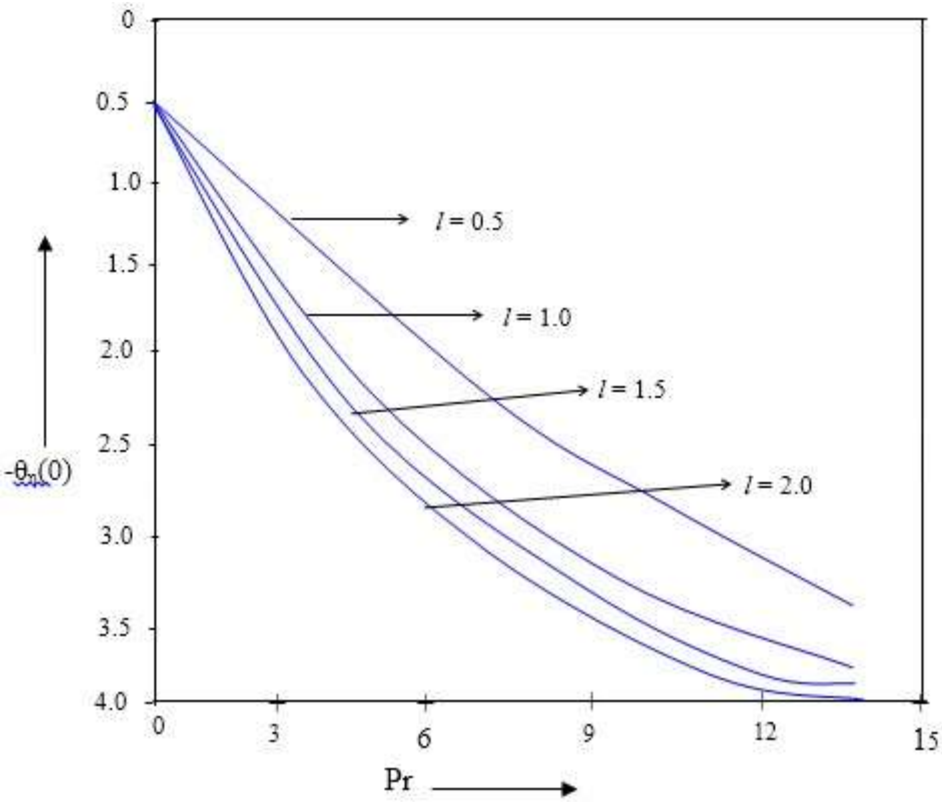

Fig6. Graph of dimensionless temperature distribution $\theta_\eta(0)$ ***Vs. Prandtl number Pr for*** k_1***=0.2, Q=0.5, Re = 100 and 4 sets of values of*** u_{wm} ***and*** $u_{\delta m}$

ISSN: 2277-9655
Impact Factor: 4.116
CODEN: IJESS7

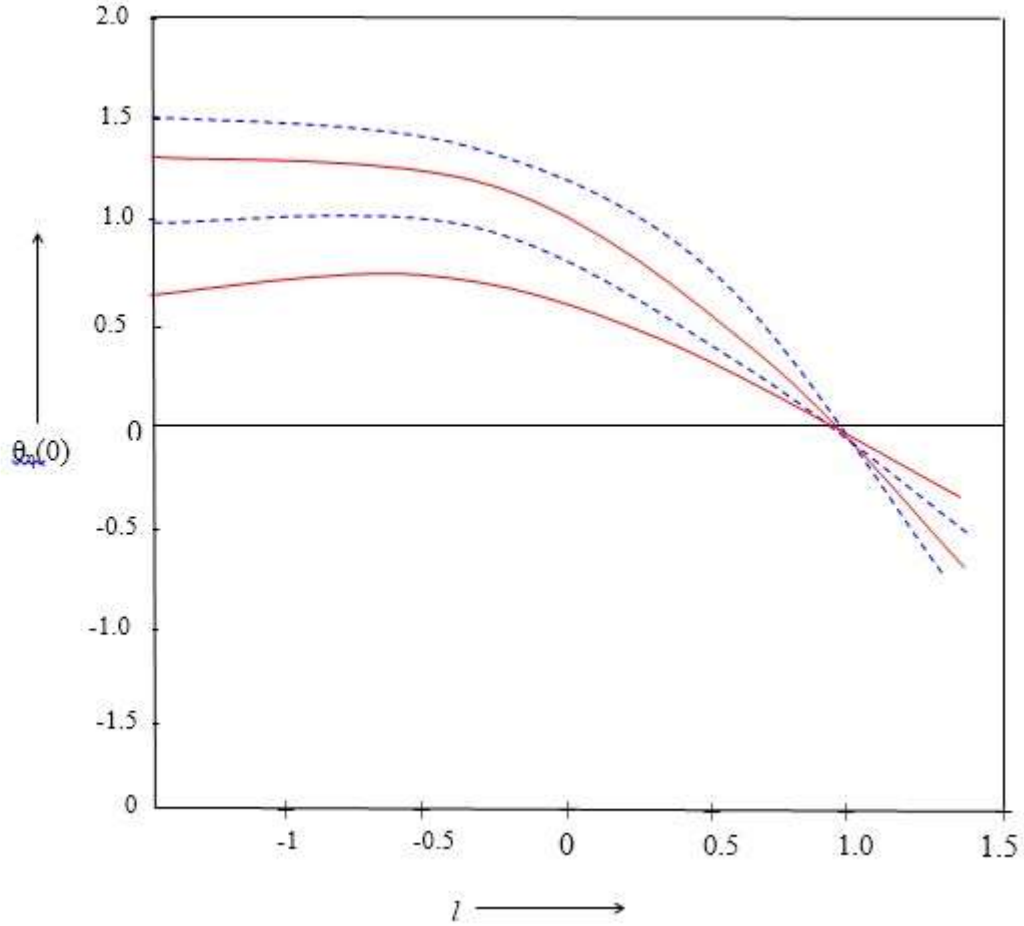

Fig7. Graph of wall temperature gradient $\theta_\eta(0)$ Vs. characteristic length l and $k_2 = 0.2$, Q = 0.5, Pr= 7

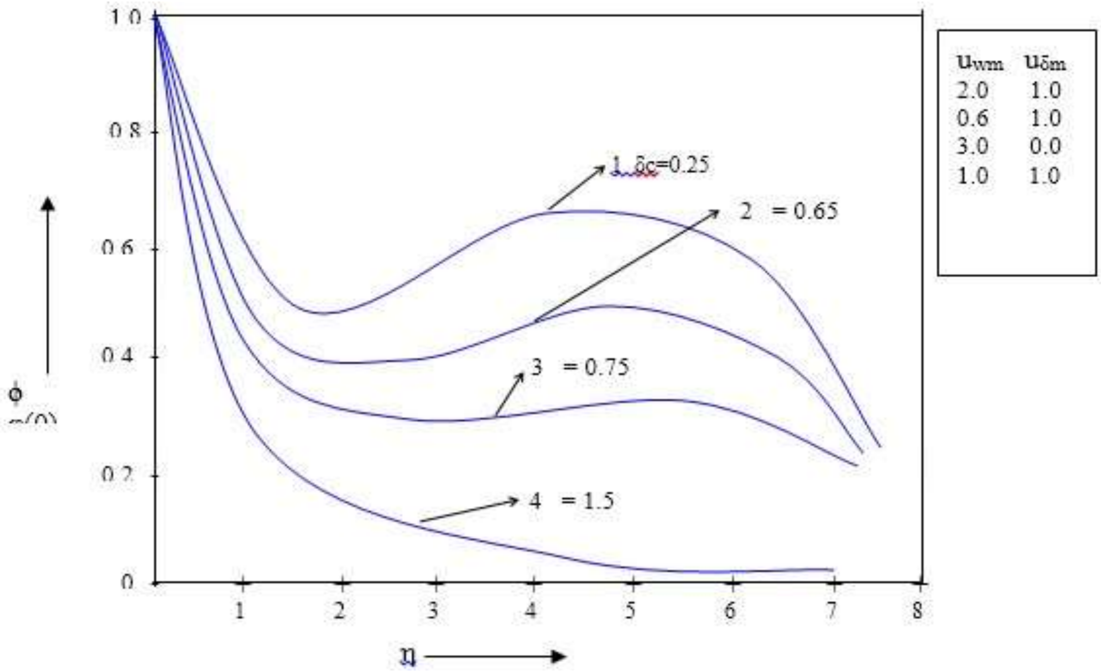

Fig8. Graph of concentration profiles $\varphi(\eta)$ Vs. η for $k_1 = 0.2$, for different values of Schimidt number Sc, Re = 100 α = 0.375

ISSN: 2277-9655
Impact Factor: 4.116
CODEN: IJESS7

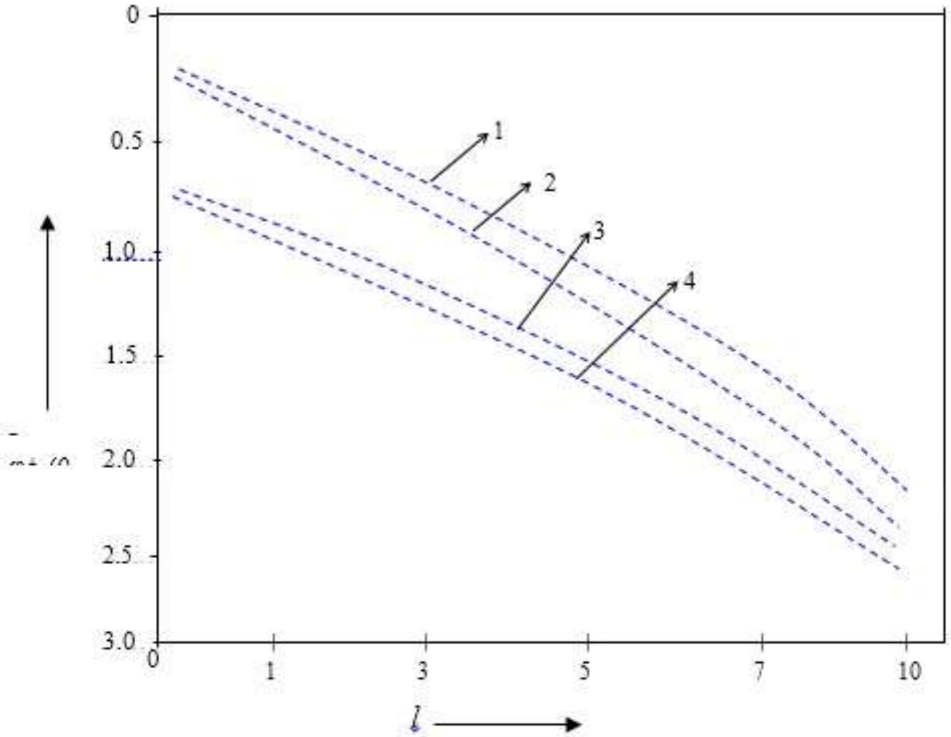

Fig 9. Graph of WALL concentration gradient -φ'(0) Vs. wall concentration parameter l. Sc = 0.65, Re = 100

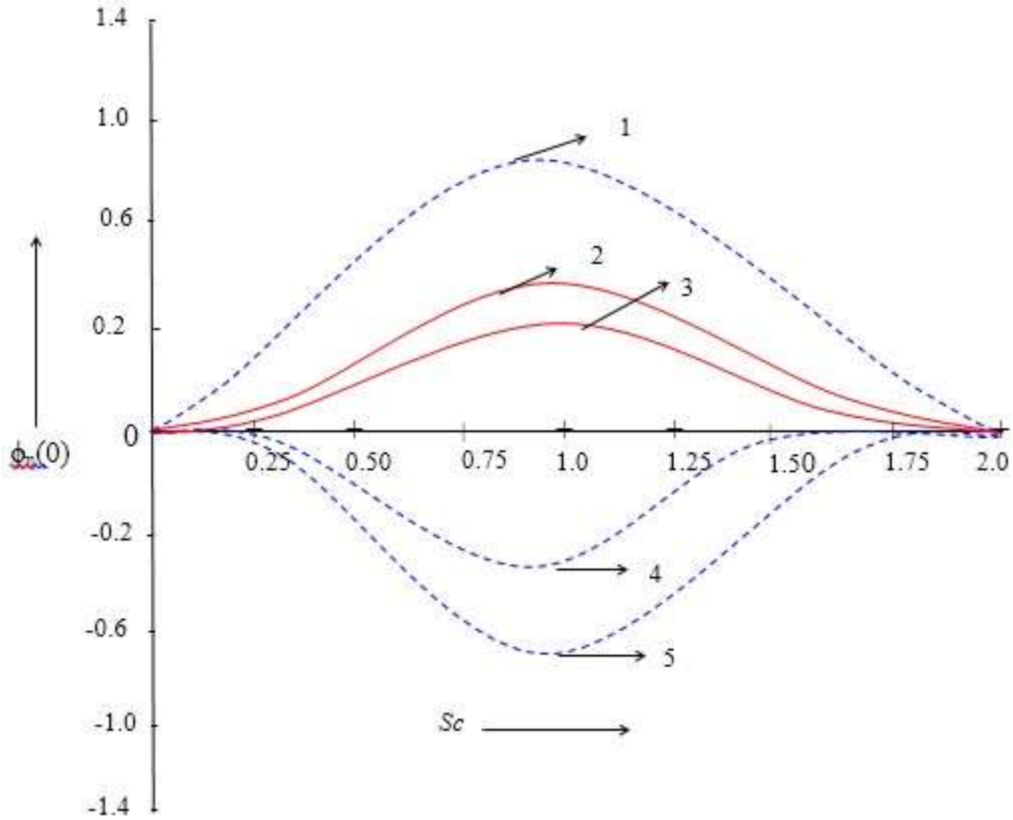

Fig10. Graph of wall concentration gradient $\theta_\eta(0)$ Vs. Schimidt number Sc for Re = 100, l = 1 and k_1 = 0.2

ISSN: 2277-9655
Impact Factor: 4.116
CODEN: IJESS7

CONCLUSIONS

Exact boundary layer similarity solutions are studied for the visco-elastic flow, heat and mass transfer characteristics on a continuous sheet extruded in a cross-cooling stream.

1. The value of skin-friction co-efficient for a given value of Reynolds number depends not only on the normalized velocity difference $| u_{um}-u_{\delta m} |$, but also on the sheet and the cooling stream.
2. For the same Prandtl and Reynolds numbers and the same normalized velocity difference, the heat transfer co-efficient is larger for the range $u_{um} > u_{\delta m}$ than $u_{um} < u_{\delta m}$.
3. For the same Schimidt and Reynolds number the mass transfer co-efficient is larger for the case $u_{um} > u_{\delta m}$ than $u_{um} < u_{\delta m}$.
4. Formation of thin thermal boundary layer and concentration boundary layer is observed far away from the plate.
5. The flow of heat becomes faster when the Prandtl number increases.
6. An increase in Schimidt number results in lowering the concentration distribution steadily.

REFERENCES

[1] B.C. Sakiadis: Boundary layer behavior on continuous solid surfaces I. Boundary layer equations for two dimensionless and axisymmetric flow. AICh. E. Journal, 7 (1961) 26-28.
[2] P.D. McCormack and L.J. Crane : Physical fluid dynamics, Academic press, New York, 1973.
[3] S.K. Khan and E. Sanjayanand : Visco-elastic boundary layer flow and heat transfer over an exponential stretching sheet, Int. J. Heat Mass transfer, 48 (2009) 1534-1542.
[4] R. Cortell : A note on flow and heat transfer of a visco-elastic fluid over a stretching sheet. Int. J. Non-linear Mechanics, 4 (2006) 78-85.
[5] R.C. Battaller : Visco-elastic fluid flow and heat transfer over a stretching sheet under the effects of a non-uniform heat source, viscous dissipation and thermal radiation. Int. J. Heat Mass Transfer 50 (2007) 3152-3162.
[6] K. Vajravelu and A. Hadjinicolaou : Heat transfer in a viscous fluid over a stretching sheet with viscous dissipation and internal heat generation, Int. Comm. Heat Mass Transfer, 20 (1993) 417-430.
[7] T.C. Chaim : Magnetohy drodhynamic heat transfer over a non-isothermal stretching sheet. Acta. Mech. 122 (1977) 169-179.
[8] M. Sajid, T. Hyaat and S. Asghar : Non-similar analytic solution for MHD flow and heat transfer in third order fluid over a stretching sheet. Int. J. Heat Mass Transfer 50 (2007) 1723-1736.
[9] S.S. Tak and A. Lodha : flow and heat transfer due to a stretching porous surface in presence of transverse magnetic field.
[10] B. Ganga, S.P. Anjalidevi and Kayalvizhi : Non-linear hydromagnetic flow and heat transfer due to a stretching porous surface with prescribed heat flux and viscous dissipation effects. Proceedings of National Conference (2007) 107-117.
[11] S.P. Arijalidevi and B. Ganga : Effects of viscous and Joules dissipation on MHD flow, heat and mass transfer past a stretching porous surface embedded in a porous medium. Non linear Analytical Modelling and Control, 14, No. 3, (2009) 303-314.
[12] I-Chung Liu : Flow and heat transfer of an electrically conducting fluid of second grade over a stretching sheet subject to a transverse magnetic field. Int. J. of Heat and Mass Transfer 47 (2004) 4427-4437.
[13] B. Siddappa and S. Abel : Non-Newtonian flow past a stretching Plate. ZAMP 36 (1985) 890-892.
[14] H.I. Anderson ; R.O. Hansen and B. Hol Medal : Diffusion of chemically reactive species from a stretching sheet. Int. J. Heat Transfer. 37 (4) (1994). 659-664.
[15] Subhas Abel and P.H. Veena : Visco-elastic fluid flow and heat transfer in a porous medium over a stretching sheet. Int. J. Non-linear Mech. 33 (1998) 531-540.
[16] S. Abel; P.H. Veena; K. Rajagopal and V.K. Pravin : Non-Newtonian magneto-hydrodynamic flow over a stretching surface with heat and mass transfer. Int. J. Non-linear Mech. 39 (2004) 1067-1078.
[17] S. Abel; P.H. Veena ; Visco-elastic fluid flow and heat transfer in a porous medium over a stretching sheet.Int. J. Nonlinear Mechanics, Vol. 33, No. 3, PP 531-543.
[18] I.A. Hassanian : Flow and heat transfer on a continuous flat surface moving in a parallel free stream of power law fluid. Appl. Math. Modelling 20 (1996) 779-781.
[19] M.S. Sarma and B.N. Rao : Heat transfer in a visco-elastic fluid over a stretching sheet. J. Math. Anal. Appl. 222 (1998) 268-275.
[20] K. Vajravelu and T. Ropper : Flow and heat transfer in a second grade fluid over a stretching sheet. Int. J.Non-linear Mech. 34 (1999) 1031-1036.

[21] I.A. Hassanian : Flow and heat transfer from a continuous surface in a parallel free stream of visco-elastic second order fluid. Appl. Sci. Res. 49 (1992) 335-344.

[22] I.A. Hassanian : Similarity solutions for flow and heat transfer of a visco-elastic fluid over a stretching sheet extruded in a cross cooling stream. ZAMM 82 (2002) 409-419.

[23] A.K. Neil : Note on similarity solutions for viscous flow over an impermeable and non-linearly stretching sheet. Int.J. Non-linear Mech 46 (2011) 1090-1091.

[24] A. Raptis and C. Perdikis : Viscous flow over a non-linearly stretching sheet in the presence of chemical reaction and magnetic field. Int. J. non-linear Mech. 41 (2006) 527-529.

[25] B.D. Coleman and W. Noll : An approximation theorm for functional with applications in continuum mechanics. Arch. Rat. Mech. Anal. 6 (1760) 355-370.

[26] J.E. Dunn and K.R. Rajagopal : Fluids of differential type, a critical review and thermodynamic analysis. Int. J. Engg. Sci. 33 (1995) 689-729.

[27] Abromowitz and L.A. Stegun : Hand book of mathematical functions 55. National Bureau of standards/Amer. Math Soc. Providance R I. 1972.